

The efficacy of new colchicine derivatives and viability of the T-Lymphoblastoid cells in three-dimensional culture using ^{19}F MRI and HPLC-UV *ex vivo*

Dorota Bartusik^{a,b,*}, Boguslaw Tomanek^{a,b,c,d}, Erika Lattová^{e,f}, H  l  ne Perreault^e, Jack Tuszynski^{g,h}, Gino Fallone^{b,d}

^a National Research Council Canada, Institute for Biodiagnostics (West), 3330 Hospital Drive NW, Calgary, Alberta, Canada T2N 4N1

^b Cross Cancer Institute, Medical Physics Department, 11560 University Ave, Edmonton, Alberta, Canada T6G 1Z2

^c Polish Academy of Sciences, Institute of Nuclear Physics, Radzikowskiego 152, 31-342 Krak  w, Poland

^d University of Alberta, Oncology Department, 11560 University Ave, Edmonton, Alberta, Canada T6G 1Z2

^e University of Manitoba, Department of Chemistry, 144 Dysart Road, Winnipeg, Manitoba, Canada R3T 2N2

^f Slovak Academy of Sciences, Centre for Glycomics, 842 38 Bratislava, Slovakia

^g Cross Cancer Institute, Experimental Oncology Department, 11560 University Ave, Edmonton, Alberta, Canada T6G 1Z2

^h University of Alberta, Department of Physics, 11322 - 89 Avenue, Edmonton, Alberta, Canada T6G 2G2

ARTICLE INFO

Article history:

Received 6 May 2009

Available online 3 August 2009

Keywords:

Colchicine

Human T-Lymphoblastoid

Three-dimensional culture

^{19}F Magnetic resonance imaging

High performance liquid chromatography

coupled with Ultra Violet

ABSTRACT

The paper describes *ex vivo* applications of colchicine derivatives for the treatment of human T-Lymphoblastoid (CEM) cells. Moreover, the role of the substitutions of ring **A** at **C-1** and **C-7** side chain of colchicine analogues was probed by the synthesis and examination of their effects on the three-dimensional (3-D) CEM cells' growth. The CEM cells were cultured in the hollow fiber bioreactor (HFB) device. We used ^1H and ^{19}F magnetic resonance imaging (MRI) to monitor changes in 3-D CEM cell culture. ^{19}F MRI was used for visualization of the cellular uptake of new fluorine derivatives. Before and after treatment CEM cells profile was investigated with high performance liquid chromatography (HPLC-UV).

Copyright    2009 Published by Elsevier Inc. All rights reserved.

1. Introduction

Colchicine (Fig. 1 (1)), has been widely used in immune-mediated diseases [1,2]. The effects associated with the frequent occurrence of drug resistance have prompted the search for new colchicine derivatives. Moreover, recent studies have showed that colchicine inhibits leukocyte-endothelial cell adhesion [3] and T-cells activation [4] by binding to intracellular tubulin monomers, which prevents their polymerization [5]. Thus, colchicine has the potential to impair the process of antigen recognition and may inhibit the cancer cells' growth.

In our experiments, the three-dimensional (3-D) cell cultures of T-Lymphoblastoid (CEM) cells were treated with novel colchicine and fluorinated colchicine derivatives. We monitored the cells' growth in the Hollow Fiber Bioreactor (HFB) device using magnetic resonance imaging (MRI), which enabled to visualize treatments

with both colchicine and fluorinated colchicines derivatives using ^1H and ^{19}F MRI, respectively. While conventional ^1H MRI detects the signal from proton of mobile water in tissue, ^{19}F MRI detects intracellular uptake of fluorine containing drugs. The natural ^{19}F abundance is too low for ^{19}F MRI detection, therefore the uptake of fluorine derivatives of colchicine in cells can be observed without any additional contrast agents.

Several studies have shown that colchicine derivatives with functionalized side chain at **C-7** position are promising for treatment of lymphocytic leukemia [6,7]. Therefore we synthesized fluorinated derivatives of colchicine with the modifications in positions **C-1** and **C-7**. Moreover, MRI technique used in this study was suitable for multiple, repeated measurements to observe dynamic changes in response to treatment and provided noninvasive *ex vivo* characteristics of the 3-D tumor.

2. Materials and methods

2.1. Chemicals and reagents

Colchicine, N-[(7S)-1,2,3,10-tetramethoxy-9-oxo-5,6,7,9-tetrahydrobenzo[ ]heptalen-7-yl] acetamide and all chemical com-

Abbreviations: CEM, human T-Lymphoblastoid; EIMS, electron impact mass spectrometry; HFB, hollow fiber bioreactor; HPLC-UV, high performance liquid chromatography coupled with Ultra Violet; MR, magnetic resonance; MRI, magnetic resonance imaging.

* Corresponding author. Address: National Research Council Canada, Institute for Biodiagnostics (West), 3330 Hospital Drive NW, Calgary, Alberta, Canada T2N 4N1. Fax: +1 780 432 8615.

E-mail address: Dorota.Bartusik@gmail.com (D. Bartusik).

pounds used to the synthesis of colchicines derivatives were purchased from Sigma–Aldrich (Oakville, ON).

2.2. Synthesis

2.2.1. Preparation of *N*-[(7*S*)-2,3,10-trimethoxy-1-((methyl)carbonyloxy)-9-oxo-5,6,7,9-tetrahydrobenzo[α]heptalen-7-yl]acetamide (2) and *N*-[(7*S*)-1-hydroxy-2,3,10-trimethoxy-9-oxo-5,6,7,9-tetrahydrobenzo[α]heptalen-7-yl]acetamide (3)

Compounds (**2**) and (**3**) were obtained by a method described by Pontakis et al. [8], as shown in Fig. 1.

2.2.2. Preparation of *N*-[(7*S*)-1-((ethyl)carbonyloxy)-2,3,10-trimethoxy-9-oxo-5,6,7,9-tetrahydrobenzo[α]heptalen-7-yl]acetamide (4) and *N*-[(7*S*)-1-(((methyl)ethyl)carbonyloxy)-2,3,10-trimethoxy-9-oxo-5,6,7,9-tetrahydrobenzo[α]heptalen-7-yl]acetamide (5)

1 mmol of derivative (**3**) was dissolved in dry pyridine and 1 mmol of propionyl chloride for preparation of (**4**) or isobutyryl chloride for preparation of (**5**) was added at 0 °C. The solution was allowed to stand overnight and then diluted with 10 mL of water and extracted with ethyl acetate (2 × 10 mL). The organic layer was washed with 5 mL of brine, dried with Na₂SO₄ and concentrated to 3 mL. Compounds (**4**) and (**5**) presented in Fig. 2 were crystallized from CH₂Cl₂.

2.2.3. Preparation of *N*-[(7*S*)-1-(ethoxy)-2,3,10-trimethoxy-9-oxo-5,6,7,9-tetrahydrobenzo[α]heptalen-7-yl] acetamide (6); *N*-[(7*S*)-1-((ethoxy)-1-methyl-2,3,10-trimethoxy-9-oxo-5,6,7,9-tetrahydrobenzo[α]heptalen-7-yl] acetamide (7); *N*-[(7*S*)-2,3,10-trimethoxy-9-oxo-1-(propanoxy)-5,6,7,9-tetrahydrobenzo[α]heptalen-7-yl]acetamide (8); *N*-[(7*S*)-2,3,10-trimethoxy-9-oxo-1-((prop(2-en)oxy)-5,6,7,9-tetrahydrobenzo[α]heptalen-7-yl]acetamide (9); *N*-[(7*S*)-2,3,10-trimethoxy-9-oxo-1-((phenyl)methoxy)-5,6,7,9-tetrahydrobenzo[α]heptalen-7-yl]acetamide (10); *N*-[(7*S*)-2,3,10-trimethoxy-9-oxo-1-(((3-methoxy)propane)oxy)-5,6,7,9-tetrahydrobenzo[α]heptalen-7-yl]acetamide (11); *N*-[(7*S*)-2,3,10-trimethoxy-9-oxo-1-((phenyl(3-chloro)methoxy)-5,6,7,9-tetrahydrobenzo[α]heptalen-7-yl]acetamide (12); *N*-[(7*S*)-2,3,10-trimethoxy-9-oxo-1-((pyridine(3))yl)-5,6,7,9-tetrahydrobenzo[α]heptalen-7-yl]acetamide (13); *N*-[(7*S*)-2,3,10-trimethoxy-9-oxo-1-((phenyl(2-chloro)methoxy)-5,6,7,9-tetrahydrobenzo[α]heptalen-7-yl] acetamide (14); *N*-[(7*S*)-2,3,10-trimethoxy-9-oxo-1-(((phenyl(4-chloro)methoxy)-5,6,7,9-tetrahydrobenzo[α]heptalen-7-yl] acetamide (15); *N*-[(7*S*)-2,3,10-trimethoxy-1-((methyl)cyclohexane)-9-oxo-5,6,7,9-tetrahydrobenzo[α]heptalen-7-yl] acetamide (16)

One millimole of derivative (**3**) was dissolved in 2.5 mL of sodium hydroxide solution and was cooled to 0 °C. 1 mmol of bromide derivatives (e.g. 1-bromoethane for preparation of (**6**), 2-methoxy-1-bromoethane for (**7**), 1-bromopropane for (**8**), 3-bromoprop-1-ene for (**9**), ((bromo)methyl)benzene for (**10**), 1-methoxy-2-bromoethane for (**11**), 1-bromo-3-chlorobenzene for (**12**), 3-((bromo)methyl)pyridine for (**13**), 1-bromo-1-chlorobenzene for (**14**), 1-bromo-4-chlorobenzene for (**15**), 1-((bromo)methyl) cyclohexane for (**16**)) was dissolved in 3.5 mL acetone and each solution was allowed to stand for 15 h, then 25 mL of alkaline water was added. Chloroform (2 × 10 mL) was used to extract the compounds, while washing was effected with 15 mL of water. The organic layers were dried with Na₂SO₄ and concentrated to 3 mL. The compounds (**6**–**16**) were crystallized from 10 mL of CH₂Cl₂. The syntheses of (**6**–**16**) are presented in Fig. 3.

2.2.4. General procedure for the preparation of *N*-deacetyl-*N*-(*N*-trifluoroacetyl aminoacyl) colchicine

Three millimoles of appropriate derivative (**6**–**16**) dissolved in methanol (50 mL) and 2 M HCl (25 mL) were heated at 90 °C with simultaneous stirring for 1 day. Next, the reaction mixture was cooled and neutralized with NaHCO₃. Products (**17**–**27**) were ex-

tracted with 10 mL of CH₂Cl₂ and washed with brine. The extracts were dried over Na₂SO₄ and concentrated to 3 mL. The deacetylated compounds (**17**–**27**) were crystallized from 10 mL of CH₂Cl₂.

One millimole of deacetylated compound (**17**–**27**) and *N*-trifluoroacetyl amino acid (1 mmol) was dissolved at room temperature in CH₂Cl₂ (6 mL). *N*-trifluoroacetyl amino acid was *N*-trifluoroacetyl glycine that was prepared from glycine by protection at the nitrogen atom with the trifluoroacetyl group [9]. As condensing compound 0.5 mmol of dicyclohexylcarbodiimide (DCC) was used. After 2 h, the suspension was cooled to 0 °C and filtrated. Products (**28**–**38**) were chromatographed on silica gel column eluting with dichloromethane/methanol (1:0–0:1). Crystallization of (**28**–**38**) were performed with dichloromethane: ethyl ether (1:1).

2.3. Cell cultures

CEM cells (American Type Culture Collection, Manassas, VA) were maintained in tissue culture flasks and cultured as monolayer in 20 mL of RPMI media containing 10% Fetal Bovine Serum (FBS). When the number of cells in the culture flask reached 5–6 × 10⁶ cells/mL, the culture was harvested and then inoculated into fifteen Hollow Fiber Bioreactors (HFB, Fiber Cells System Inc., Frederick, MD) and continuously cultured in 37 °C and 5% CO₂. The media circulating within the HFB cartridge and polysulfone tubing, at flow rate of 14 mL/min, bring oxygen and nutrients to cells and remove CO₂ and other waste. HFB device with 1 cm diameter consists of a single, hydrophilic and polysulfone fiber with 0.1 μm diameter pores. We used collagen solution to create an extracellular matrix between the cells and the fiber. The polysulfone fiber was coated with protein by flushing with 10 mL of coating solution containing 1 mg of collagen per 1 mL Phosphate Buffered Saline (PBS). Due to perfusion, the HFB absorbed sufficient oxygen from the reservoir with fresh media to keep cells alive. The perfusion medium was changed weekly when the glucose level reached 2 g/L measured with a glucometer. The number of cells was determined manually with a hemacytometer chamber (Hausser Scientific, Horsham, PA) using Trypan blue exclusion method [10].

2.4. Cell treatment

To establish IC₅₀, 4 × 10⁴ CEM cells/mL in six well microplates were used to determine the activity of (**1**–**38**) compounds. Solutions of the treated media with (**1**–**38**) were prepared using: 1 nM, 10 nM, 20 nM, 100 nM, 500 nM and 1000 nM of (**1**–**38**) placed in a 1.5 mL glass vials and dissolved in 10 μL of dimethyl sulfoxide. 10 μL of dimethyl sulfoxide was the solvent for each (**1**–**38**) derivative. Once dissolved, the dimethyl sulfoxide/(**1**–**38**) appropriate mixtures were added to the media and incubated overnight in 37 °C. The cells were exposed to (**1**–**38**) and incubated for 72 h. After treatment, 0.4% (w/v) Trypan blue dye solution was added and cell viability was then determined using a hemacytometer chamber. Moreover, CEM cells were treated with 10 μL of dimethyl sulfoxide alone and viability after 72 h was also examined.

To treat 3-D cultures in the HFB device for 72 h we selected (**6**), (**13**), (**28**) and (**35**) compounds, because for these colchicine derivatives the cells' growth was inhibited over 50% for relatively low concentration of 20 nM. For each treatment with 1000 nM of (**6**), (**13**), (**28**) and (**35**) three HFBs were used (*n* = 12 for treatment; *n* = 3 for control). Viability of cells removed from the HFB was measured with Trypan blue.

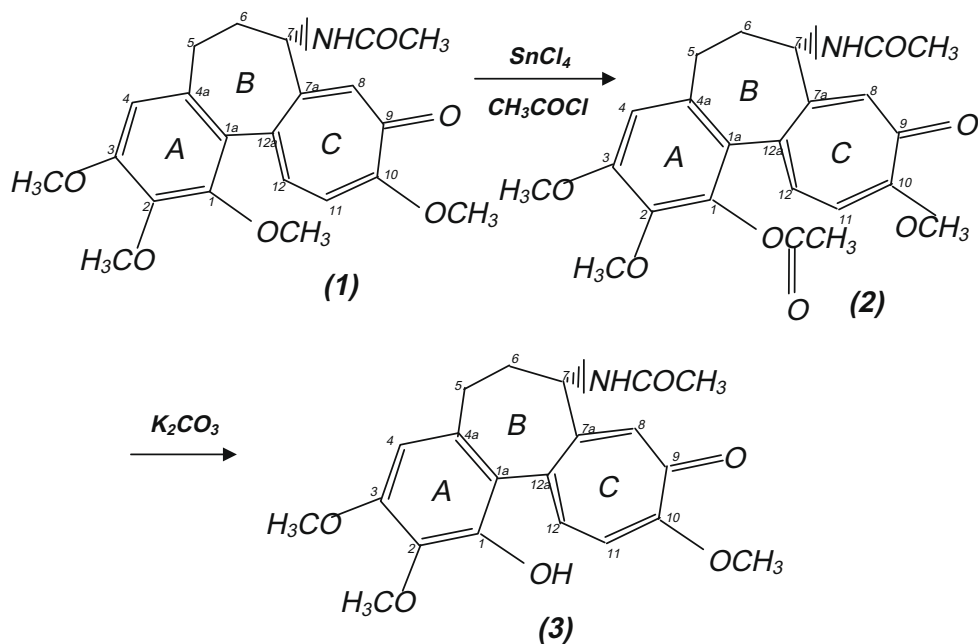
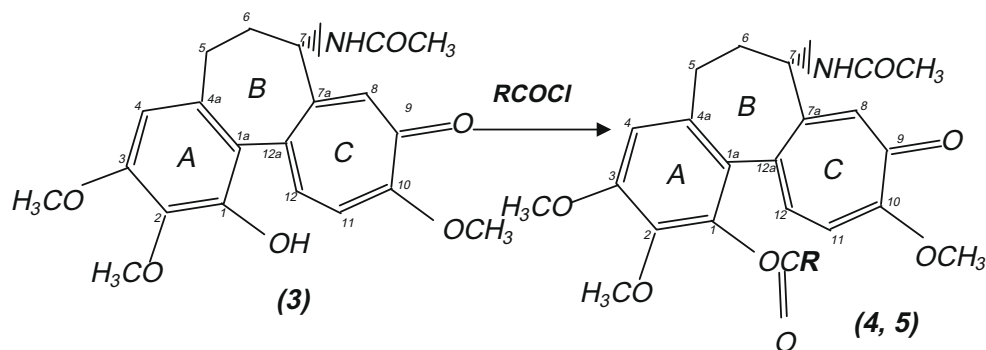


Fig. 1. Structures of the compounds (1), (2) and (3).

2.5. MRI

All MRI experiments were performed using a 9.4 Tesla (T) with 21 cm bore magnet (Magnex, UK) and TMX console (NRC-IBD, Canada). Images were acquired using double (^{19}F and ^1H) tuned transmit/receive Radio Frequency (RF) volume coil operating at 376 MHz and 400 MHz corresponding to ^{19}F and ^1H Larmour frequency at 9.4 T, respectively. For ^1H MRI, a spin echo pulse sequence was used with Echo Time (TE)/Repetition Time (TR) = 16.5/5000 ms. ^{19}F MRI was performed with Inversion Recovery (IR) spin echo method with Inversion Time (IT) of 400 ms and TE/TR = 16.5/5000 ms. For imaging of HFBs, axial slices with 1 mm thickness were defined perpendicular to the HFB's long axis and field of view was set to 3×3 cm, matrix size of 256×256 resulting in a resolution of $117 \times 117 \mu\text{m}$ for ^1H and ^{19}F MRI. ^1H MR images were collected before drug introduction and after 72 h of exposure to (6), (13), (28) and (35).

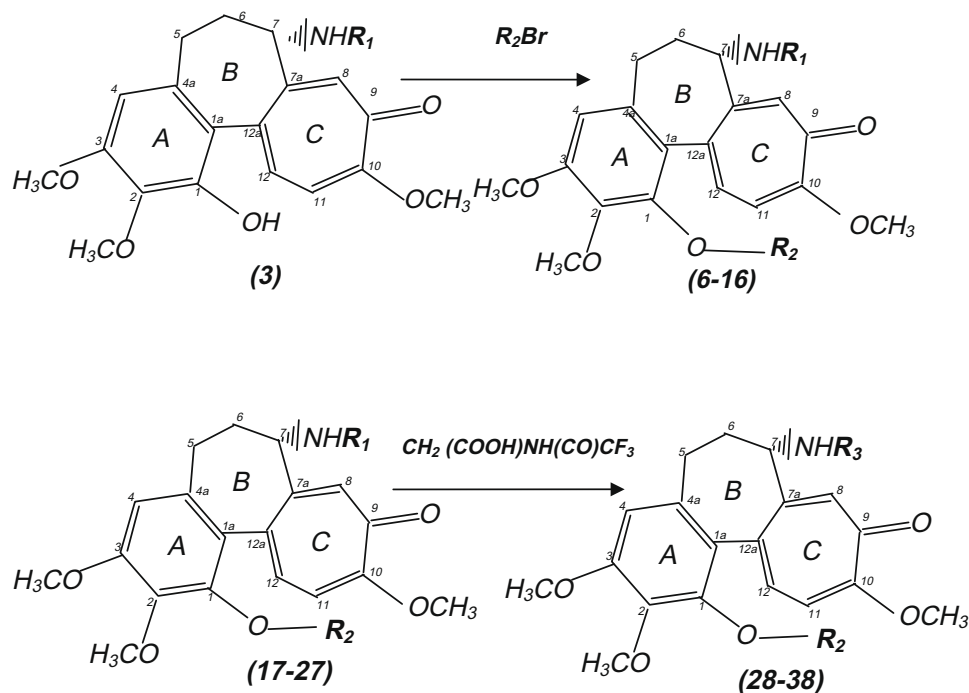
^{19}F MR imaging was performed to determine the intracellular ^{19}F SI of (28) and (35) on the cell cultures in HFBs devices. To optimize the intracellular uptake of (28) and (35) the phantoms consisting of HFB tubes filled with 10^3 cells, 10^4 cells, 10^5 cells, 10^6 cells, 10^7 cells, 10^8 cells and 10^9 cells and 1 nM, 10 nM, 20 nM, 100 nM, 500 nM and 1000 nM of (28) or (35) were used. It is already known, that ^{19}F SI is linearly related with the amount of ^{19}F molecules taken up by cells [11]. Therefore, the linear regression was used to find the ^{19}F SI dependence on treated cell numbers. The ^{19}F SI measured from axial slices of tubes filled with pure (28) and (35) without cells were considered as 100% of SI. Percentage change in SI (^{19}F SI (% change)) was normalized to the SI of pure (28) and (35) with the use of the following equation: ^{19}F SI (% change) = $[(U - L)/U] \times 100\%$, where (U) was pure (28) and (35) and L = ^{19}F SI of (28) or (35) in each samples containing different cell numbers. To measure intracellular uptake of drug without ^{19}F background from treated media, the cells in HFB device after



(4) R = CH_3CH_2

(5) R = $(\text{CH}_3)_2\text{CH}$

Fig. 2. Scheme of the preparation of (4–5).



(6) $R_2 - CH_2CH_3$; $R_1 - (CO)CH_3$	(17) $R_2 - CH_2CH_3$; $R_1 - H$	(28) $R_2 - CH_2CH_3$; $R_3 - (CO)CH_2NH(CO)CF_3$
(7) $R_2 - CH(CH_3)_2$; $R_1 - (CO)CH_3$	(18) $R_2 - CH(CH_3)_2$; $R_1 - H$	(29) $R_2 - CH(CH_3)_2$; $R_3 - (CO)CH_2NH(CO)CF_3$
(8) $R_2 - CH_2CH_2CH_3$; $R_1 - (CO)CH_3$	(19) $R_2 - CH_2CH_2CH_3$; $R_1 - H$	(30) $R_2 - CH_2CH_2CH_3$; $R_3 - (CO)CH_2NH(CO)CF_3$
(9) $R_2 - CH_2CH=CH_2$; $R_1 - (CO)CH_3$	(20) $R_2 - CH_2CH=CH_2$; $R_1 - H$	(31) $R_2 - CH_2CH=CH_2$; $R_3 - (CO)CH_2NH(CO)CF_3$
(10) $R_2 - CH_2(C_6H_5)$; $R_1 - (CO)CH_3$	(21) $R_2 - CH_2(C_6H_5)$; $R_1 - H$	(32) $R_2 - CH_2(C_6H_5)$; $R_3 - (CO)CH_2NH(CO)CF_3$
(11) $R_2 - CH_2CH_2OCH_3$; $R_1 - (CO)CH_3$	(22) $R_2 - CH_2CH_2OCH_3$; $R_1 - H$	(33) $R_2 - CH_2CH_2OCH_3$; $R_3 - (CO)CH_2NH(CO)CF_3$
(12) $R_2 - CH_2(C_6H_4)\text{-m-Cl}$; $R_1 - (CO)CH_3$	(23) $R_2 - CH_2(C_6H_4)\text{-m-Cl}$; $R_1 - H$	(34) $R_2 - CH_2(C_6H_4)\text{-m-Cl}$; $R_3 - (CO)CH_2NH(CO)CF_3$
(13) $R_2 - CH_2(\text{p-C}_6\text{H}_4\text{N})$; $R_1 - (CO)CH_3$	(24) $R_2 - CH_2(\text{p-C}_6\text{H}_4\text{N})$; $R_1 - H$	(35) $R_2 - CH_2(\text{p-C}_6\text{H}_4\text{N})$; $R_3 - (CO)CH_2NH(CO)CF_3$
(14) $R_2 - CH_2(C_6H_4)\text{-o-Cl}$; $R_1 - (CO)CH_3$	(25) $R_2 - CH_2(C_6H_4)\text{-o-Cl}$; $R_1 - H$	(36) $R_2 - CH_2(C_6H_4)\text{-o-Cl}$; $R_3 - (CO)CH_2NH(CO)CF_3$
(15) $R_2 - CH_2(C_6H_4)\text{-p-Cl}$; $R_1 - (CO)CH_3$	(26) $R_2 - CH_2(C_6H_4)\text{-p-Cl}$; $R_1 - H$	(37) $R_2 - CH_2(C_6H_4)\text{-p-Cl}$; $R_3 - (CO)CH_2NH(CO)CF_3$
(16) $R_2 - CH_2(C_6H_{11})$; $R_1 - (CO)CH_3$	(27) $R_2 - CH_2(C_6H_{11})$; $R_1 - H$	(38) $R_2 - CH_2(C_6H_{11})$; $R_3 - (CO)CH_2NH(CO)CF_3$

Fig. 3. Scheme of the syntheses (6–38).

treatment were washed with fresh media. The media were pumping with flow rate of 14 mL/min and 5 mL sample from media reservoir was taken after every washing to check ^{19}F SI. The washing of cells was repeated until ^{19}F SI of media was too low for measurements with ^{19}F MRI at 9.4 T. Data analysis was proceeded with post-processing software MAREVISI (NRC-IBD, Canada).

2.6. HPLC-UV

Digested cell samples were fractionated with a Gold HPLC chromatograph system equipped with a Gold 166 Ultra Violet (UV) Detector and 32-Karat software (Beckman-Coulter, Mississauga, ON). For reversed-phase HPLC, a Vydac 218 TP54 Protein & Peptide C18 analytical column, 300 Å pore size, 0.46 cm \times 25 cm (Separation Group, Hesperia, CA) was used. The chromatograph was equipped with a Rheodyne injector (5 μL). UV detection was per-

formed at 245 nm. Eluent A consisted of 5% acetonitrile (ACN) water solution and eluent B of 0.01% trifluoroacetic acid in 95% ACN water solution. A linear gradient from 5% to 70% ACN was applied over 60 min.

2.7. Statistical analysis

Results were expressed as a mean \pm SD. Differences between groups at each time-point were identified by one-way Anova. Statistical comparison between two independent variables was determined by two-way Anova with Dunnett's correction performed post hoc to correct multiple comparisons. The p -values < 0.05 were considered statistically significant. All data reported here are from sets of three separate experiments. Error bars in all graphs represent the standard error of the mean. Data were analyzed using the Sigma Stat Soft software (Chicago, IL).

3. Results

Colchicine analogues synthesized and tested for their ability to inhibit CEM cell growth *ex vivo* were separated into three groups and are presented in Figs. 1–3. The syntheses of the colchicine derivatives started with the conversion of known classical colchicine structure to ester or ether structure at the position C-1. The hydrolysis of (2) in the presence of K_2CO_3 produced compound (3) (Fig. 1) with 71% yield. The esterification of (3) afforded ester derivatives (4–5) as shown in Fig. 2. The class of compounds (6–16) were obtained by etherification of (3) (Fig. 3). Among these compounds, fluorine derivatives (28–38) were synthesized using (17–27) as started compounds (Fig. 3).

The 3-D cell cultures in the HFB device reached 10^9 CEM cells/mL after 4 weeks. The 72 h incubations of cells with (6–16) and (28–35) decreased cells viability and showed the ability of the analogues to accumulate and interact within cells. The observed IC_{50} of the cells' growth inhibition using colchicine analogues are summarized in Fig. 4. The analogues of (6–16) exhibited a similar effect with main value $IC_{50} = 13 \pm 1$ nM. However, (28–35) analogues showed a higher decreases in cells viability and main $IC_{50} = 7 \pm 2$ nM. The observed IC_{50} suggested a lower capacity to antagonize cells' growth for (6–16) derivatives than (28–35). The fluorinated analogues (28–35) were the most effective compounds in all studied derivatives (1–38). After the preliminary test of (17–27) we did not perform viability studies using these derivatives, because the observed effects did not show decreases of cells' viability higher than the precursor (1). However, the compounds (6) and (13) showed significant changes in IC_{50} values. Based on these results, we selected (6) and (13) as well as their fluorinated analogues (28) and (35) for the studies in HFB device. The influence of the investigated compounds on 3-D CEM cell growth was confirmed with cell viability binding assays. As shown in Fig. 5, the compounds (6) or (13) and fluorinated analogues (28) or (35) were able to induce high growth inhibition effect in HFB cultures. Viability of the control (untreated) cells during culture was $93 \pm 2\%$. Cells treated with $10 \mu\text{L}$ of dimethyl sulfoxide did not show any decreases in growth.

To observe the 3-D cells aggregation in the HFB device, the cells before and after treatment with (6), (13), (28) and (35) were imaged with the use of ^1H MRI. The ^1H images allowed to monitor the localization of cells around the fiber device, thus providing anatomical images of the cultures. Fig. 6A and Fig. 6B are ^1H images with the resolution of $117 \times 117 \mu\text{m}$ and present the cross-section of the entire HFB device with cells treated with (6) and (13),

respectively. The viable cells are visible with ^1H MRI and their number decreased during time exposure to the drugs, which corresponds to decrease of cells volume observed on the ^1H image. The data indicate that the regions of cells with low signal intensities (SI) (more darker) are the regions with more dead cells, as examined with Trypan blue. The loss of intracellular water in region of dead cells confirmed the differences in SI. The total region of cells visible with ^1H MRI decreased for $25 \pm 3\%$ and $35 \pm 6\%$ as compared to regions before treatment with (6) and (13), respectively. These data imply that the flow of medium through the HFB center provides a nutrient source and clearance of waste products and that the cells are with high densities close to the fiber. Accordingly, the region of cells with high densities before treatment, possesses more viable cells after treatment. Particularly, the number of cells before and after treatment proved that close to the fiber the density of cells was 10% higher as compared to others region of HFB.

^{19}F MR images were collected in treated cells at the same imaging session and the same geometry that were used to ^1H MR images. The treatment effect on ^{19}F MR images was the increased ^{19}F SI due to increased cellular uptake of fluorine drug and dead cells, therefore ^{19}F SI was measured for the cells treated in HFB device with fluorine derivatives (28) and (35). Following previously published recommendation, ^{19}F SI was measured directly from axial slice of HFB device [12]. Moreover, ^{19}F MRI selectively visualizes only intracellular fluorine uptake with no background and shows distribution of derivatives in cell cultures. As proved by viability assay, the cells visible with ^{19}F MRI are nonviable cells while examined by Trypan blue. The distribution of cells can be measured by MRI and in the HFB device, the cells possessed density distribution. The significantly higher number of cells was killed in the regions where cells' density was high. Fig. 6C and D are ^{19}F images and showed uptake of (28) and (35) derivatives of colchicines in dead cells. No ^{19}F signal was observed from extracellular media, for instance compounds that have not been taken up by cells because fresh media was flushed right after treatment. SI was measured as a regional signal and then the mean value was calculated.

The data presented in Figs. 7 and 8 illustrated the optimization process of *ex vivo* applications of (28) and (35). The ^{19}F SI was linear with respect to ^{19}F content in known numbers of cells. Moreover, both figures, Figs. 7 and 8, illustrated that: the concentration of emulsions can be quantified based on the ^{19}F SI and the number of targeted cells can be counted based on ^{19}F SI values. Therefore, we estimated the number of CEM cells labeled with ^{19}F -derivatives of colchicines in HFB devices. Study showed that, within 72 h cells exposure to 1000 nM of (28) and (35), the num-

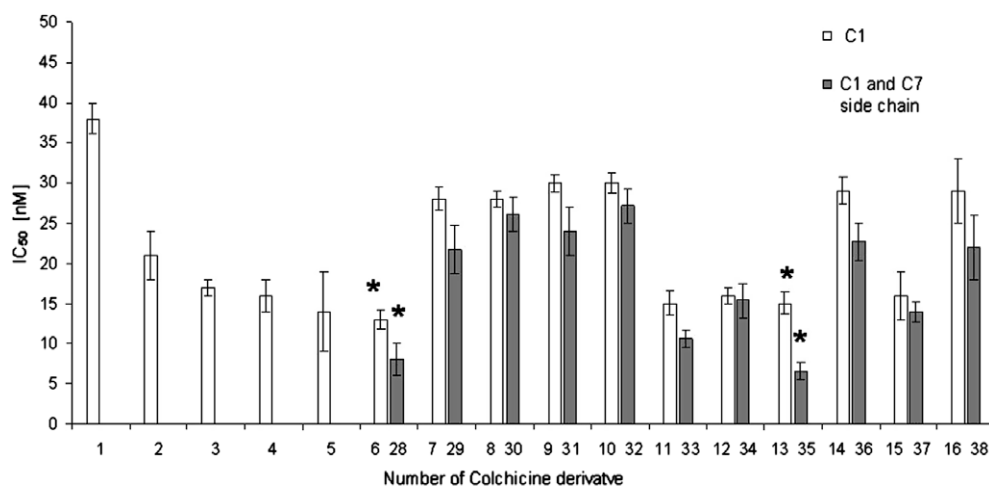


Fig. 4. IC_{50} values of (1–38).

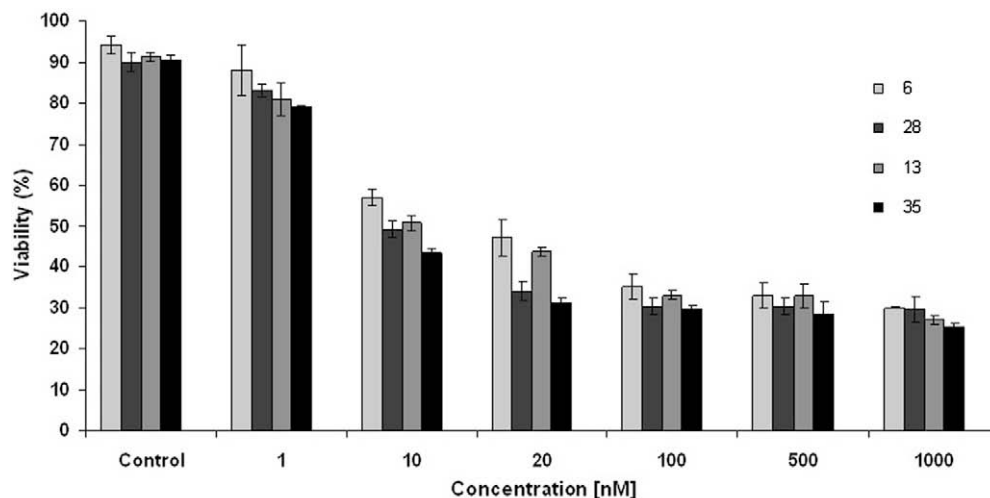


Fig. 5. Viability of cells treated with (6), (13), (28) and (35).

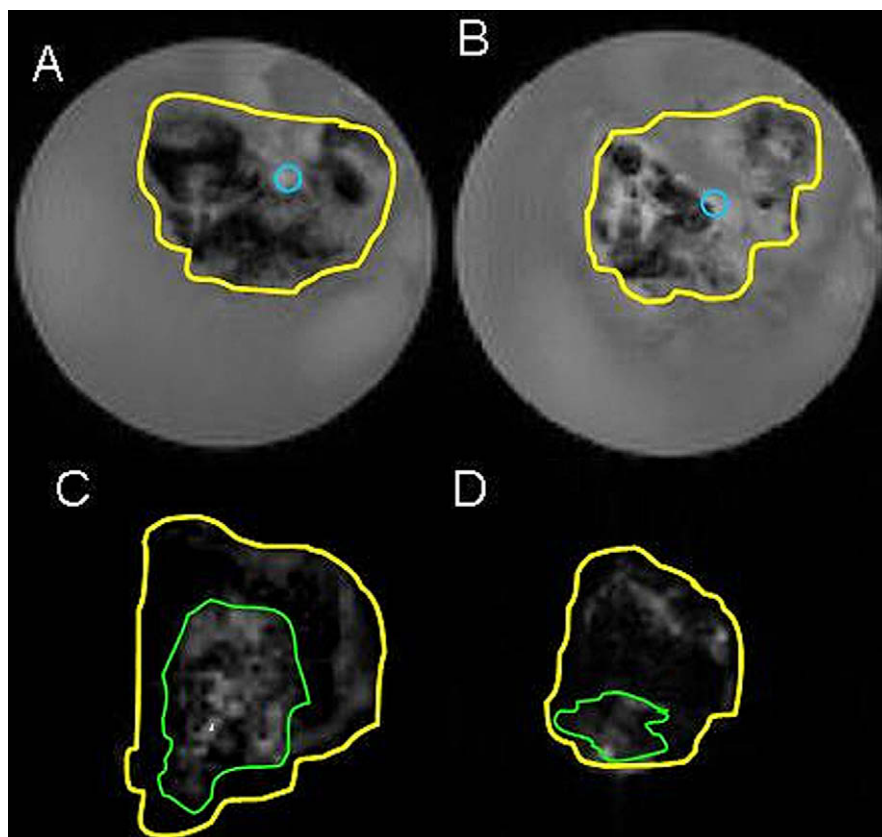


Fig. 6. ^1H MRI of CEM cells treated with (6) (A); ^1H MRI of cells treated with (13) (B); ^{19}F MRI of cells treated with (28) (C); ^{19}F MRI of cells treated with (35) (D). The yellow solid line indicated the cells region (A–D), the blue solid line indicated the fiber (A, B) and the green solid line indicated region with higher uptake of fluorine derivatives (C, D). The scale of (A–D) to original image is 3:1.

bers of viable cells decreased from 10^9 cells/mL to 3.45×10^8 cells/mL and from 10^9 cells/mL to 2.9×10^8 cells/mL, respectively. The mean ^{19}F SI of the cells treated with (28) increased during treatment and corresponding to a mean cells concentration of 6.03×10^8 cells/mL. The mean CEM cell density in the region with lower densities corresponds to 2.4×10^8 cells/mL while the mean numbers of cells with higher cells densities corresponds to 3.5×10^8 cells/mL. At the same time the viability of cells in HFB treated with (28) was 35% and corresponding to 3.45×10^8 cells/mL viable cells in HFB.

The mean ^{19}F SI of the cells treated with (35) also increased during treatment and corresponded to a mean cells concentration of 6.9×10^8 cells/mL. The viability of cells in HFB treated with (35) was 30% and corresponded to live cells 2.9×10^8 cells/mL after 3 days of treatment. The mean CEM cell density in the region with lower densities corresponded to 1.4×10^8 cells/mL while the mean numbers of cells with higher cells densities were 4.8×10^8 cells/mL. As expected, the ^{19}F SI values were dependent on the concentration of cells and fluorine derivatives in the cells treated with (28) (Fig. 7) and (35) (Fig. 8).

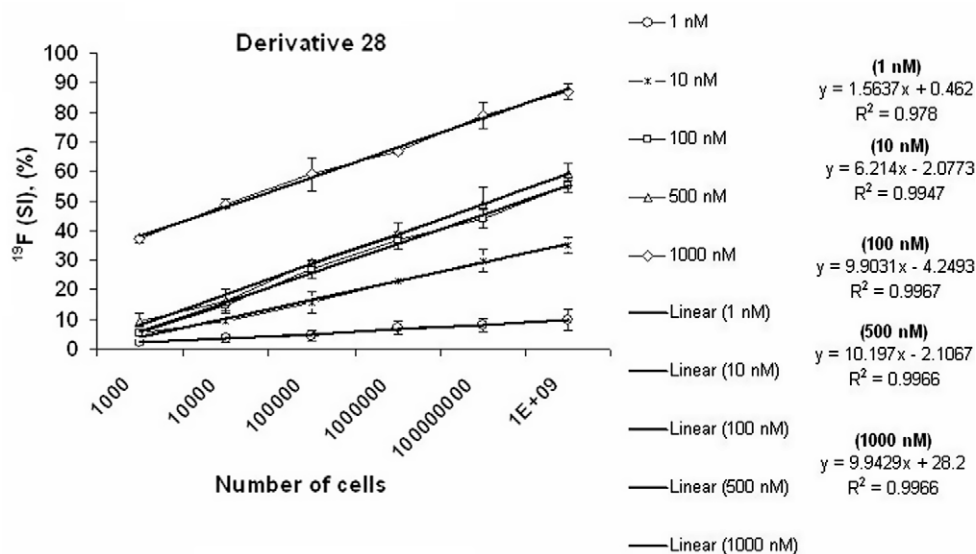


Fig. 7. Number of cells vs. increase of ¹⁹F SI for (28) (100% corresponds to SI of pure (28) without cells).

Moreover, we found, that 3-D high density cell cultures were needed for the study, due to the limited MRI sensitivity. We also found, that the HFB provides high enough concentration of cells to obtain ¹H and ¹⁹F MR images, thus the combined MRI techniques and HFB device can be used for studying fluorine drug efficacy and cells viability.

The results of the HPLC analysis of the treated CEM cells *ex vivo* are shown in Fig. 9A–E. Particularly, Fig. 9A showed fraction of untreated CEM cells. As shown in Fig. 9C and E, the cells in response to treatment with (13) and (35) expressed the minor histocompatibility complex MHC (class I) receptor eluted at 52 min. When the viability was 45% and 35%, the expression of MHC (class I) receptor was observed with intensities of 0.05 Volt (V) and 0.7 V, respectively. The exposure of cells to (6), (13) and (28) showed a new HPLC peak eluted at 23 min with low intensity, the Tn receptor (Fig. 9B–D). The signal of Tn in cells treated

with (13) had intensity 10 times higher (Fig. 9C) in 45% viable cell culture than treated with (6) in 50% viable cell culture (Fig. 9B) and with (28) in 38% viable cell culture (Fig. 9D). We assumed that signals eluted at 30–35 min were unreacted derivatives with variable intensity of 0.1 V for (28) and (35) as well as 0.35 V for (13) and 0.3 V for (6). The viability of cell cultures were higher for samples where unreacted colchicine derivatives were presented with higher intensities and were as follow: 38% ± 4 for (28), 35% ± 5 for (35), 45% ± 2 for (13) and 50% ± 4 for (6). Additional signal from cascade of apoptotic proteins was eluted at 56 min and occurred in samples treated with (28) and (35) (Fig. 9D and E). The peaks at 56 min with intensity of 0.35 V (28) and 0.2 V (35) were measured in cells with viability of 38% (28) and 35% (35). The undefined additional peaks with very low intensities, less than 0.05 V, are the metabolites of derivatives or unreacted compounds.

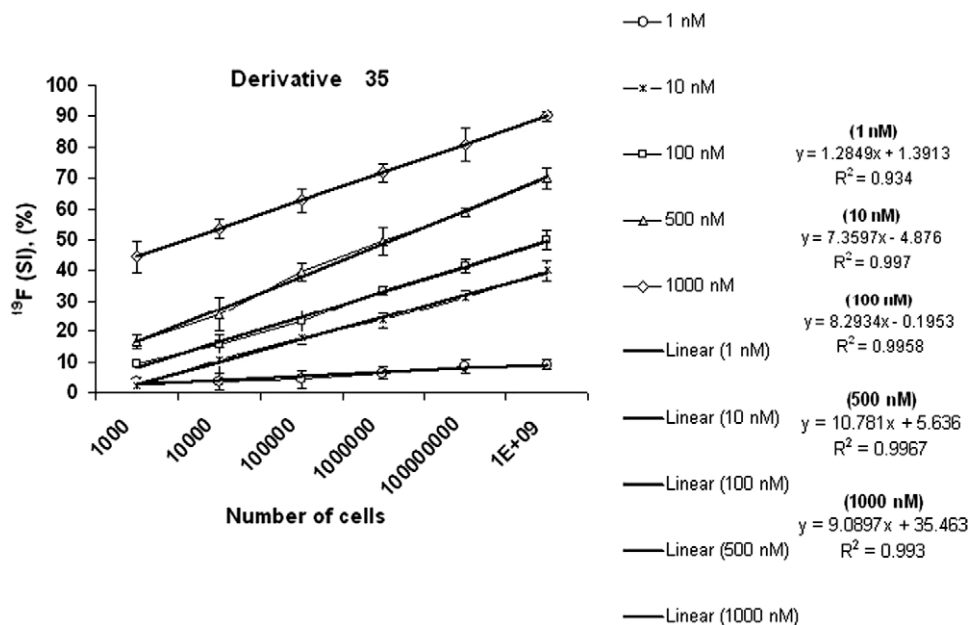


Fig. 8. Number of cells vs. increase of ¹⁹F SI for (35) (100% corresponds to SI of pure (35) without cells).

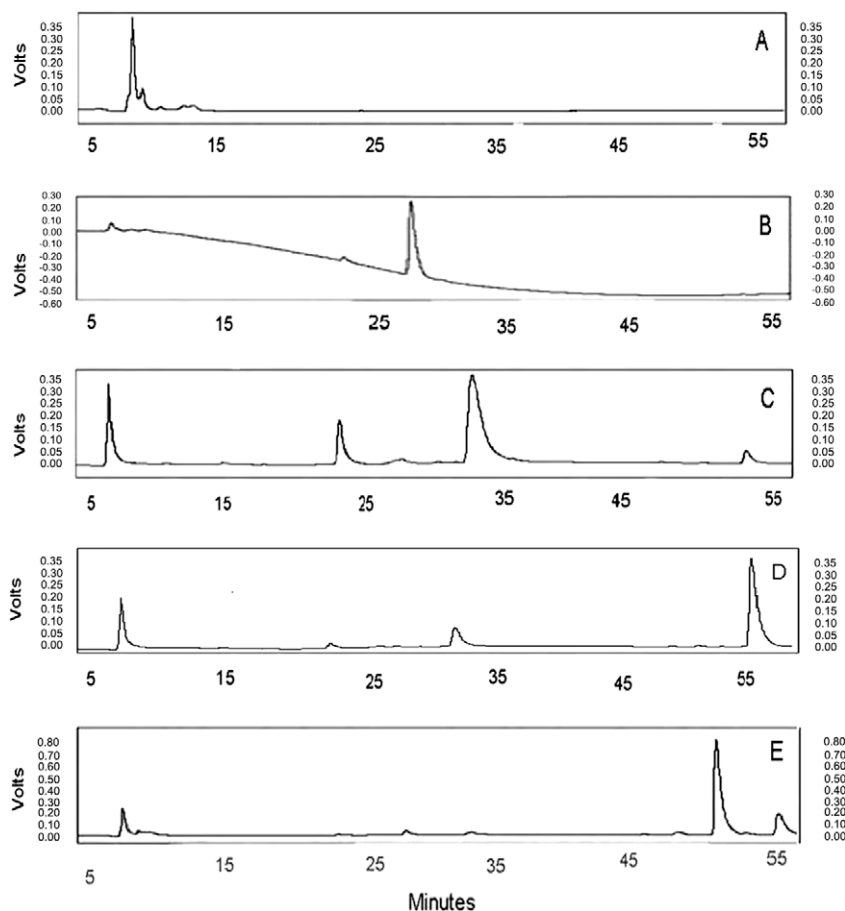


Fig. 9. HPLC chromatograms of untreated CEM cells (A); cells treated with (6) (B); cells treated with (13) (C); cells treated with (28) (D) and cells treated with (35) (E).

3.1. Analytical analysis

(2) $C_{23}H_{25}O_7N_1$; requires M, 427. Found EIMS m/e 427.1 (M+); Calcd. for $C_{23}H_{25}O_7N_1$: C, 64.63; H, 5.85; N, 3.27. Found: C, 64.64; H, 5.86; N, 3.31. (3) $C_{21}H_{23}O_6N_1$; requires M, 385. Found EIMS m/e 385.1 (M+); Calcd. for $C_{21}H_{23}O_6N_1$: C, 65.45; H, 5.97; N, 3.63. Found: C, 65.43; H, 5.99; N, 3.71. (4) $C_{24}H_{27}O_7N_1$; requires M, 441. Found EIMS m/e 441.1 (M+); Calcd. for $C_{24}H_{27}O_7N_1$: C, 65.30; H, 6.12; N, 3.72. Found: C, 65.31; H, 6.12; N, 3.72. (5) $C_{25}H_{29}O_7N_1$; requires M, 455. Found EIMS m/e 455.0 (M+); Calcd. for $C_{25}H_{29}O_7N_1$: C, 65.93; H, 6.37; N, 3.07. Found: C, 65.94; H, 6.38; N, 3.08. (6) $C_{23}H_{27}O_6N_1$; requires M, 413. Found EIMS m/e 413.1 (M+); Calcd. for $C_{23}H_{27}O_6N_1$: C, 66.83; H, 6.55; N, 23.22. Found: C, 66.82; H, 6.54; N, 23.22. (7) $C_{24}H_{29}O_6N_1$; requires M, 427. Found EIMS m/e 427.1 (M+); Calcd. for $C_{24}H_{29}O_6N_1$: C, 67.44; H, 6.77; N, 3.22. Found: C, 67.41; H, 6.73; N, 3.21. (8) $C_{24}H_{29}O_6N_1$; requires M, 427. Found EIMS m/e 427.1 (M+); Calcd. for $C_{24}H_{29}O_6N_1$: C, 67.44; H, 6.79; N, 32.78. Found: C, 67.44; H, 6.80; N, 32.77. (9) $C_{24}H_{27}O_6N_1$; requires M, 425. Found EIMS m/e 425.1 (M+); Calcd. for $C_{24}H_{27}O_6N_1$: C, 67.76; H, 6.35; N, 3.29. Found: C, 67.77; H, 6.33; N, 3.28. (10) $C_{28}H_{29}O_6N_1$; requires M, 475. Found EIMS m/e 475.2 (M+); Calcd. for $C_{28}H_{29}O_6N_1$: C, 70.73; H, 6.10; N, 2.94. Found: C, 70.87; H, 5.92; N, 2.93. (11) $C_{24}H_{29}O_7N_1$; requires M, 443. Found EIMS m/e 443.1 (M+); Calcd. for $C_{24}H_{29}O_7N_1$: C, 65.01; H, 6.54; N, 3.16. Found: C, 65.02; H, 6.53; N, 3.11. (12) $C_{28}H_{28}O_6N_1Cl_1$; requires M, 509. Found EIMS m/e 509.1 (M+); Calcd. for $C_{28}H_{28}O_6N_1Cl_1$: C, 66.01; H, 5.05; N, 2.75. Found: C, 71.05; H, 6.12; N, 2.95. (13) $C_{27}H_{28}O_6N_2$; requires M, 476. found EIMS m/e 476.1 (M+); Calcd. for $C_{27}H_{28}O_6N_2$: C, 68.06; H, 5.88; N, 5.88; Found: C, 68.09; H, 5.86; N, 5.89. (14)

$C_{28}H_{28}O_6N_1Cl_1$; requires M, 509. Found EIMS m/e 509.1 (M+); Calcd. for $C_{28}H_{28}O_6N_1Cl_1$: C, 66.01; H, 5.50; N, 2.94; Cl, 6.87. Found: C, 66.03; H, 5.51; N, 2.95; Cl, 6.88. (15) $C_{28}H_{28}O_6N_1Cl_1$; requires M, 509. Found EIMS m/e 509.1 (M+); Anal. Calcd. for $C_{28}H_{28}O_6N_1Cl_1$: C, 65.01; H, 6.09; N, 3.16; Cl, 7.90. Found: C, 65.02; H, 6.07; N, 3.10; Cl, 7.92. (16) $C_{28}H_{35}O_6N_1$; requires M, 481. Found EIMS m/e 481.2 (M+); Calcd. for $C_{28}H_{35}O_6N_1$: C, 69.85; H, 7.27; N, 2.91. Found: C, 70.04; H, 7.08; N, 2.93. (17) $C_{21}H_{25}O_5N_1$; Anal. Calcd. for $C_{21}H_{25}O_5N_1$: C, 67.92; H, 7.27; N, 3.77. Found: C, 67.93; H, 7.28; N, 3.78. (18) $C_{22}H_{27}O_5N_1$ Calcd. for $C_{22}H_{27}O_5N_1$: C, 68.57; H, 7.01; N, 3.77. Found: C, 68.59; H, 7.03; N, 3.79. (19) $C_{22}H_{27}O_5N_1$; Calcd. for $C_{22}H_{27}O_5N_1$: C, 68.57; H, 7.01; N, 3.78. Found: C, 68.62; H, 7.05; N, 3.79. (20) $C_{22}H_{25}O_5N_1$; Calcd. for $C_{22}H_{25}O_5N_1$: C, 68.92; H, 6.52; N, 3.65. Found: C, 68.94; H, 6.53; N, 3.67. (21) $C_{26}H_{27}O_5N_1$; Calcd. for $C_{26}H_{27}O_5N_1$: C, 72.05; H, 6.23; N, 3.23. Found: C, 72.21; H, 6.04; N, 3.23. (22) $C_{22}H_{27}O_6N_1$; Calcd. for $C_{22}H_{27}O_6N_1$: C, 65.83; H, 6.73; N, 3.49. Found: C, 65.82; H, 6.73; N, 3.48. (23) $C_{26}H_{26}O_5N_1Cl_1$; Calcd. for $C_{26}H_{26}O_5N_1Cl_1$: C, 66.80; H, 5.56; N, 2.99; Cl, 7.49. Found: C, 66.93; H, 5.34; N, 3.01; Cl, 7.53. (24) $C_{22}H_{26}O_5N_1$; Calcd. for $C_{22}H_{26}O_5N_1$: C, 68.75; H, 6.77; N, 3.64. Found: C, 81.26; H, 6.78; N, 3.66. (25) $C_{26}H_{26}O_5N_1Cl_1$; Calcd. for $C_{26}H_{26}O_5N_1Cl_1$: C, 66.80; H, 5.56; N, 2.99; Cl, 7.49. Found: C, 66.81; H, 5.55; N, 2.98; Cl, 7.48. (26) $C_{26}H_{26}O_5N_1Cl_1$; Calcd. for $C_{26}H_{26}O_5N_1Cl_1$: C, 66.80; H, 5.56; N, 2.99; Cl, 7.49. Found: C, 66.81; H, 5.57; N, 2.85; Cl, 7.51. (27) $C_{26}H_{33}O_5N_1$; Calcd. for $C_{26}H_{33}O_5N_1$: C, 76.53; H, 7.51; N, 3.18. Found: C, 76.22; H, 7.32; N, 3.20. (28) $C_{25}H_{27}O_7N_2F_3$; Calcd. for $C_{25}H_{27}O_7N_2F_3$: C, 57.25; H, 5.15; N, 5.18; F, 10.85. Found: C, 57.25; H, 4.99; N, 5.34; F, 10.86. (29) $C_{26}H_{29}O_7N_2F_3$; Calcd. for $C_{26}H_{29}O_7N_2F_3$: C, 57.99; H, 5.39; N, 5.20; F, 10.59. Found: C, 56.38; H, 5.3; N, 5.3; F, 10.87. (30)

$C_{26}H_{29}O_7N_2F_3$; Calcd. for $C_{26}H_{29}O_7N_2F_3$: C, 57.99; H, 5.39; N, 5.20; F, 10.59. Found: C, 57.58; H, 5.32; N, 5.28; F, 10.59. **(31)**
 $C_{26}H_{27}O_7N_2F_3$; Anal. Calcd. for $C_{26}H_{27}O_7N_2F_3$: C, 58.20; H, 5.03; N, 5.22; F, 10.36. Found: C, 57.99; H, 5.88; N, 5.28; F, 10.55. **(32)**
 $C_{30}H_{29}O_7N_2F_3$; Calcd. for $C_{30}H_{29}O_7N_2F_3$: C, 61.43; H, 4.94; N, 4.77; F, 9.72. Found: C, 61.71; H, 4.65; N, 4.37; F, 9.49. **(33)**
 $C_{26}H_{29}O_7N_2F_3$; Calcd. for $C_{26}H_{29}O_7N_2F_3$: C, 57.99; H, 5.39; N, 5.20; F, 10.59. Found: C, 56.38; H, 5.21; N, 4.68; F, 9.55. **(34)**
 $C_{30}H_{28}O_7N_2Cl_1F_3$; Calcd. for $C_{30}H_{28}O_7N_2Cl_1F_3$: C, 58.06; H, 4.51; N, 4.50; F, 9.19. Found: C, 58.04; H, 4.29; N, 4.12; F, 8.43. **(35)**
 $C_{26}H_{28}O_7N_2F_3$; Calcd. for $C_{26}H_{28}O_7N_2F_3$: C, 58.06; H, 4.86; N, 4.69; F, 9.56. Found: C, 58.12; H, 4.87; N, 4.69; F, 9.57. **(36)**
 $C_{30}H_{28}O_7N_2Cl_1F_3$; Calcd. for $C_{30}H_{28}O_7N_2Cl_1F_3$: C, 58.06; H, 4.15; N, 4.12; F, 8.41. Found: C, 58.06; H, 4.14; N, 4.13; F, 8.40. **(37)**
 $C_{30}H_{28}O_7N_2Cl_1F_3$; Calcd. for $C_{30}H_{28}O_7N_2Cl_1F_3$: C, 58.06; H, 4.15; N, 4.12; F, 8.41. Found: C, 58.07; H, 4.18; N, 4.12; F, 9.26. **(38)**
 $C_{30}H_{35}O_7N_2F_3$; Calcd. for $C_{30}H_{35}O_7N_2F_3$: C, 60.81; H, 5.91; N, 4.72; F, 9.62. Found: C, 60.79; H, 5.67; N, 4.63; F, 9.67.

4. Discussion

Success of drug efficacy to treat cancerous tissues is highly dependent on their interaction with cells. Currently it is evident that the efficient drug-cell interaction, accurate drug delivery, trafficking of the therapeutic and the high density cell culture should be considered for *ex vivo* studies.

In human body CEM tumor exists in 3-D environment, however, conventional monolayer cell cultures used in biological and toxicological studies are two dimensional (2-D). Recent pioneering research in the field of cancer has illustrated that 3-D culture systems can maintain *in vivo* condition, what is unavailable for 2-D cells suspension [13]. To study the treatment *ex vivo*, we employed 3-D structure of cells developed in HFB. The use of HFB allowed to obtain high density cancerous tissue, suitable for MRI monitoring of the dynamic of the cellular changes.

Colchicine derivatives with substitutions at **C-1** position of **A** ring are limited in numbers [14]. Thus **A** ring of colchicine is crucial for tubulin binding and has attracted attention for further study on tubulin-microtubule system. For tubulin binding, the size of methyl group of methoxy substituent of the **A** ring plays an important role. Substitution of methyl group from any of the three-methoxy groups with bulky groups results in manifold reduction of the potency of cancer cells to grow. As yet, use of colchicine *in vivo* has proven to be difficult, as the action has not been completely established. We showed that the effect of derivatives presented improvement of the IC_{50} values and caused tumor suppression. The lack of clinical interest in the colchicine (**1**) arises from its toxicity. However, cancer cells are significantly more vulnerable to colchicine poisoning than healthy cells. Therefore, many attempts

are made to discover more effective analogues of colchicine by modifying basic structure (**1**). Various arguments e.g. duration of the exposure to colchicine analogues (**2–38**), interaction among cells, drug metabolism may be put forward to explain the difference in cells' viability that corresponds to growth inhibition using prepared analogues. As expected, the fluorinated derivative (**28–38**) displayed the high antagonistic potency on cells growth in 3-D cultures. The use of ^{19}F provides potential tool for the study of treatment efficacy of the CEM cells. In the studied CEM cells, the ^{19}F SI increased due to ^{19}F uptake, however the cells that are successfully treated are no longer viable for trypan blue assays. Therefore, combined measurements of viability using Trypan blue and drug uptake using ^{19}F SI gave total cell number that is equal to the number of cells before treatment.

Considering the applied technique, HPLC has proven particularly effective in the determinations of apoptotic protein even in low concentrations. Moreover, reversed-phase (RP) HPLC is known as reliable method for the separation of a great number of proteins and peptides with high reproducibility. Therefore, we established a fractionation procedure to enrich less abundant proteins using RP HPLC. The cells' viability caused by apoptosis has been suggested to be a major factor in cell death in treatment of malignancies, such as lymphoma. In particular, HPLC profile explains why this nonviable cell that expresses specific receptors occurred mostly in treated cells. It has been also reported that determined Tn antigen is expressed in over 70% of human carcinoma cells [14].

Finally, the study shows, that ^{19}F MRI, HPLC-UV and Trypan blue assays are suitable for monitoring of cells' condition before and after treatments with colchicine derivatives.

References

- [1] P. Seidemann, B. Fjellner, A. Johannesson, J. Rheumatol. 14 (1987) 777–779.
- [2] J.P. Callen, J. Am. Acad. Dermatol. 13 (1987) 193–200.
- [3] S.J. Rosenman, A.A. Ganji, W.M. Gallatin, FASEB J. 5 (1991) 1603–1609.
- [4] Y.A. Mekory, D. Baram, A. Goldberg, A. Klajman, Cell. Immunol. 120 (1989) 330–340.
- [5] G.O. Borisy, E.W. Taylor, J. Cell. Biol. 34 (1967) 533–548.
- [6] A. Brossi, P.N. Sharma, L. Atwell, A.E. Jacobson, M.A. Iorio, M. Molinari, C.F. Chignell, J. Med. Chem. 26 (1983) 1365–1369.
- [7] M. Rosner, H.G. Capraro, A.E. Jacobson, L. Atwell, A. Brossi, M.A. Iorio, T.H. Williams, R.H. Sik, C.F. Chignell, J. Med. Chem. 24 (1981) 257–261.
- [8] R. Pontakis, S. Nguyen-Hoang-Nam, H. Hoellinger, L. Picha, J. Label. Compd. Radiopharm. 20 (4) (1983) 549–552.
- [9] F. Weigand, R. Geiger, Chem. Ber. 89 (1956) 647–652.
- [10] K. Takahashi, G. Loo, Biochem. Pharm. 67 (2004) 315–324.
- [11] M. Srinivas, P.A. Morel, L.A. Ernst, D.H. Laidlaw, E.T. Ahrens, Magn. Reson. Med. 58 (2007) 725–734.
- [12] J.H. Felgner, R. Kumar, C.N. Sridhar, C.J. Wheeler, Y.J. Tsai, R. Border, P. Ramsey, M. Martin, P.L. Felgner, J. Biol. Chem. 269 (1994) 2550–2561.
- [13] M.N. Kirstein, R.C. Brundage, W.F. Elmquist, R.P. Rempel, P.H. Marker, D.E. Guire, D. Yee, Breast. Cancer Res. Treat. 96 (2006) 203–301.
- [14] G.F.T. Springer, Science (Washington DC) 224 (1984) 1198–1206.